

Supplement to the article

Weather Type Reconstruction using Machine Learning Approaches

Authors: Lucas Pfister^{1,2}, Lena Wilhelm^{1,2}, Yuri Brugnara^{1,2*}, Noemi Imfeld^{1,2}, Stefan Brönnimann^{1,2}

- 5 ¹ Oeschger Centre for Climate Change Research, University of Bern, Bern, 3012, Switzerland
² Institute of Geography, University of Bern, Bern, 3012, Switzerland

*now at EMPA, Dübendorf, 8600, Switzerland

S.1 Predictor correlations

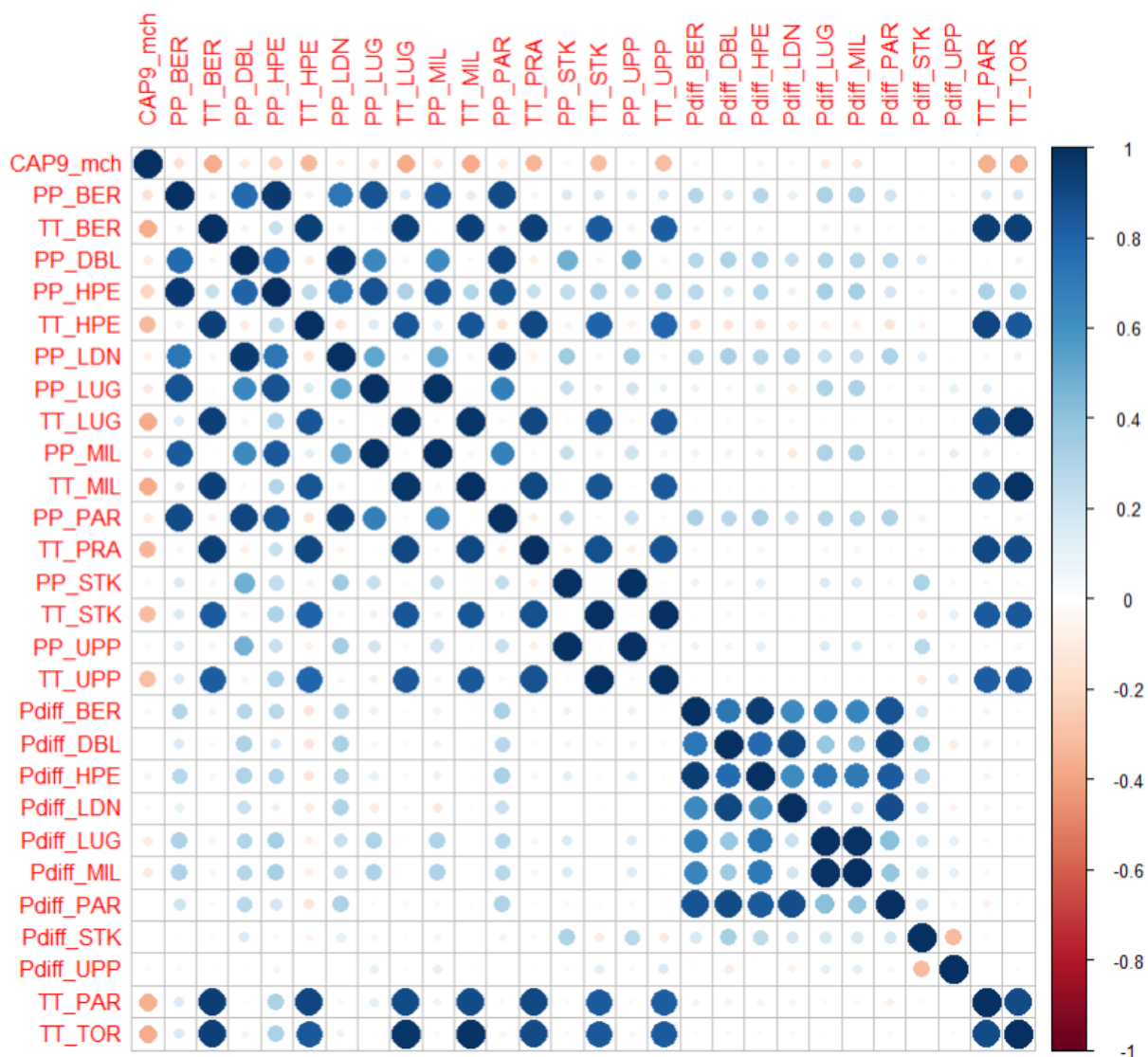


Figure S1.1: Correlations between variables used for the model comparison including the weather types (CAP9_mch). Shown are pearson correlations for the SMD station set with 11 stations as used by Schwander et al. (2017)

S.2 Multinomial logistic regression (MLG) model coefficients and fitted relationships

Table S2.1: Coefficients β_n of the six MLG predictands (PP_MIL, PP_PAR, TT_PRA, TT_STK, Pdiff_MIL and Pdiff_STK) for each CAP9 class. Class one is taken as reference. All predictands are highly significant (not shown).

Class	Intercept	PP_MIL	PP_PAR	TT_PRA	TT_STK	Pdiff_MIL	Pdiff_STK
2	686.3291	-0.0633	-0.6142	0.1239	-0.1066	-0.0765	-0.0810
3	-998.7799	1.0667	-0.0846	-0.0116	-0.0506	-0.0334	-0.0330
4	-1352.5444	0.9168	0.4126	-0.2003	0.1352	0.0356	0.0510
5	-2597.8647	2.0411	0.5076	-0.3536	0.1913	0.0164	0.0499
6	1334.6536	-0.9174	-0.4009	0.0436	-0.0416	-0.0270	-0.0285
7	2034.2208	-0.9707	-1.0427	0.2170	-0.1497	-0.1160	-0.1034
8	-4061.5719	2.9962	0.9768	-0.6759	0.3139	0.0585	0.0834
9	2957.1726	-1.7344	-1.1998	0.2361	-0.1795	-0.0607	-0.0881

10

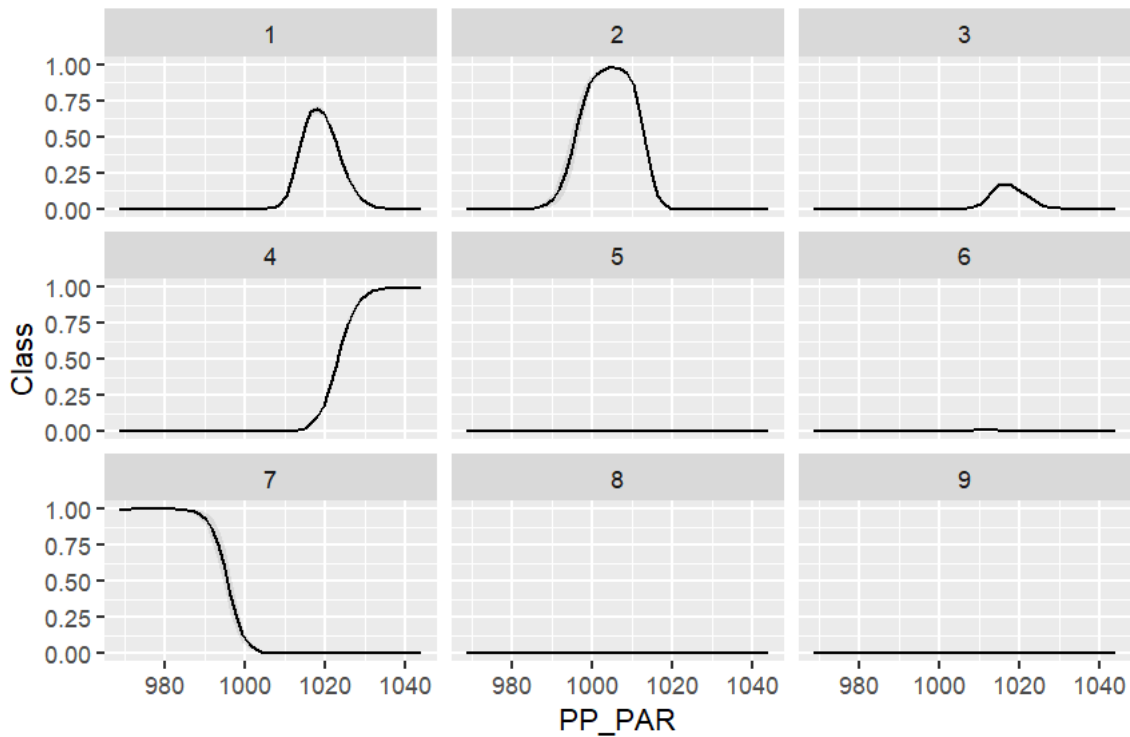


Figure S2.1: Fitted model relationships of the predictand PP_PAR per CAP9 class. The probability of the respective class (y-axes) is plotted against the values of PP_PAR in hPa (x-axes).

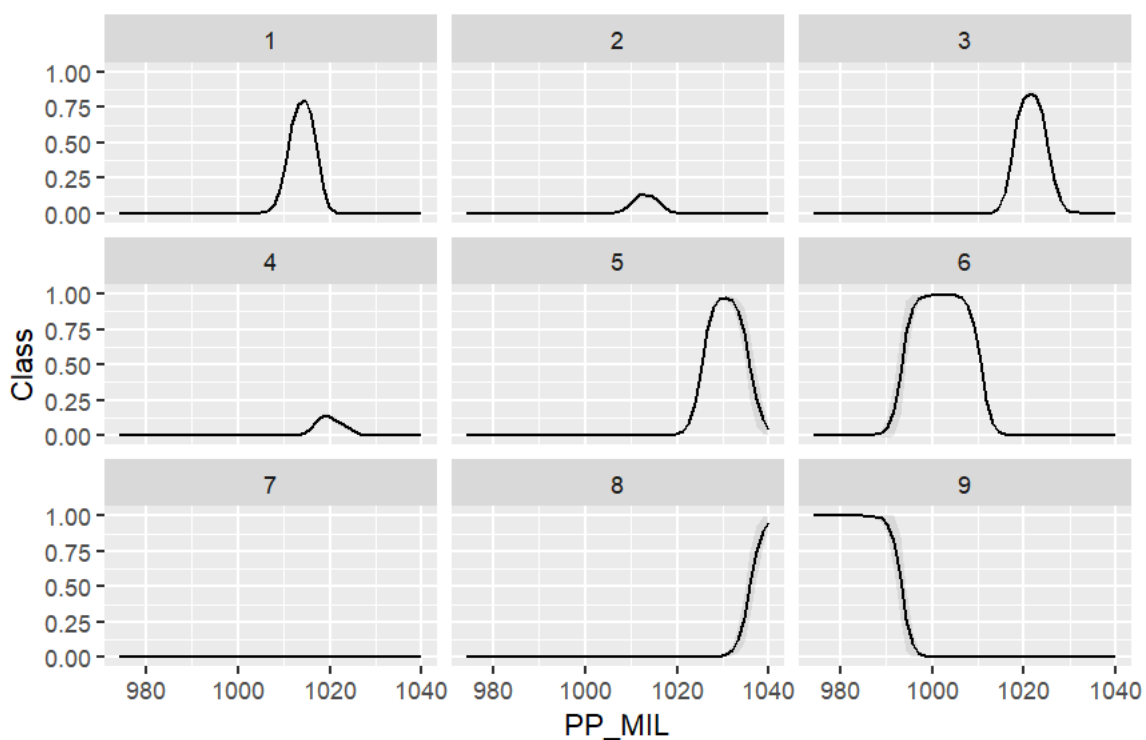


Figure S2.2: As figure S2.1, but for PP_MIL.

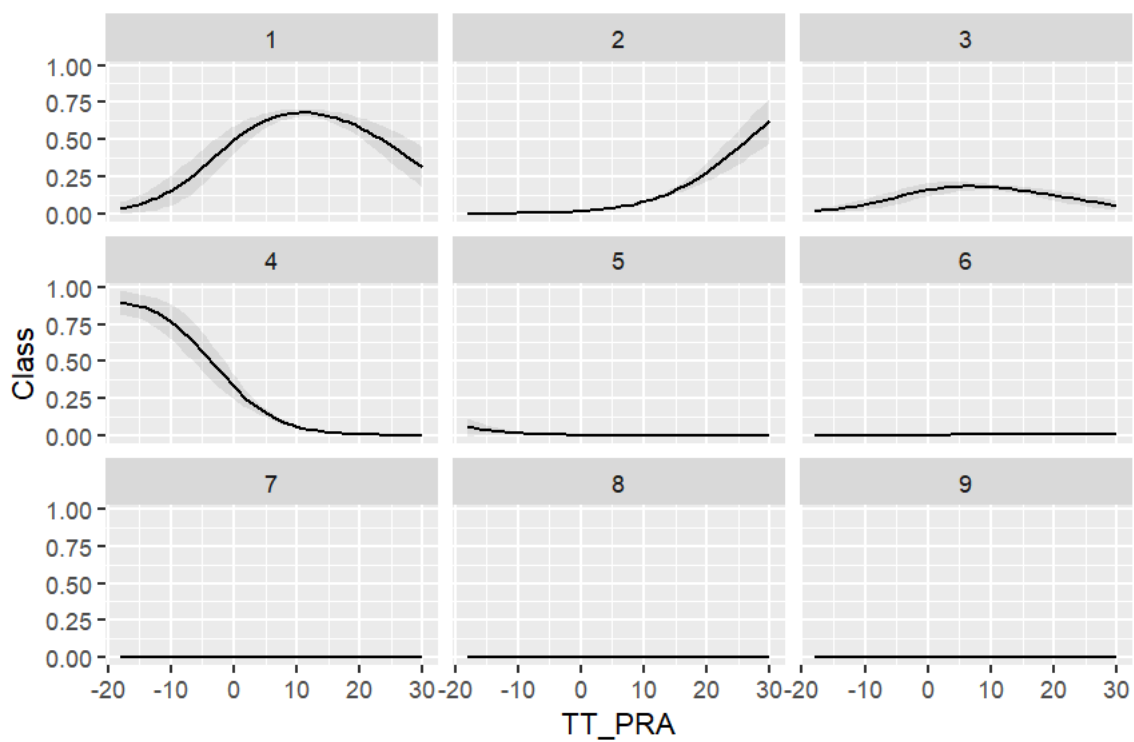
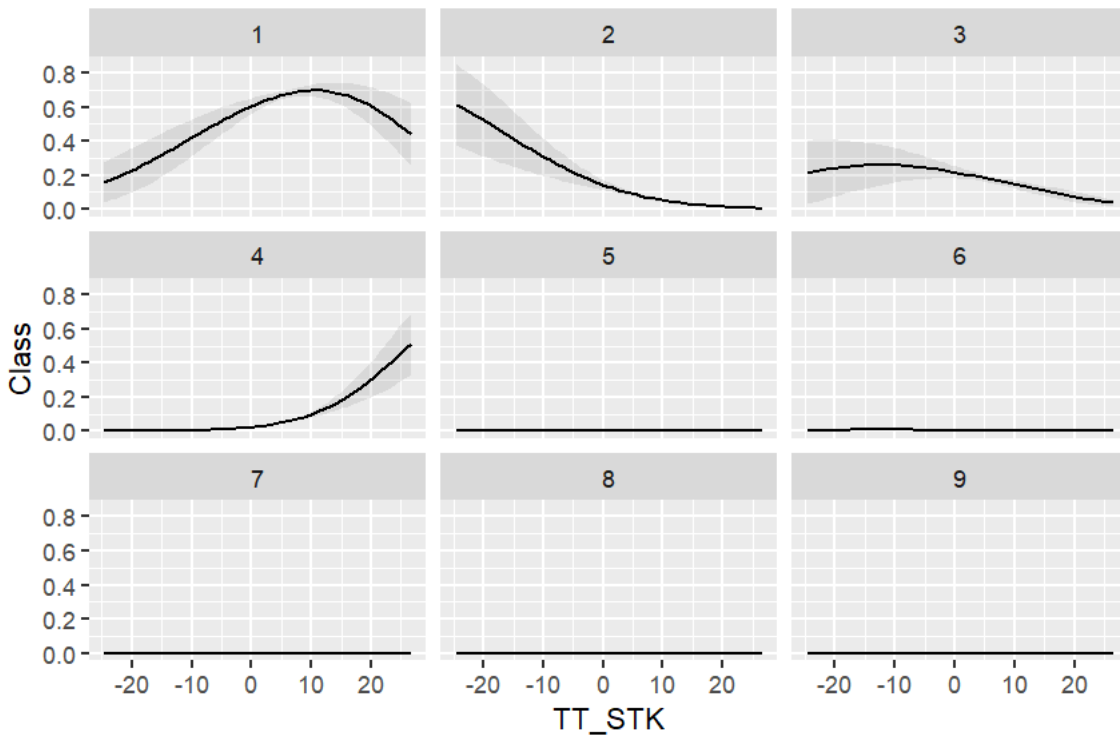


Figure S2.3: As figure S2.1, but for TT_PRA.



15

Figure S2.4: As figure S2.1, but for *TT_STK*.

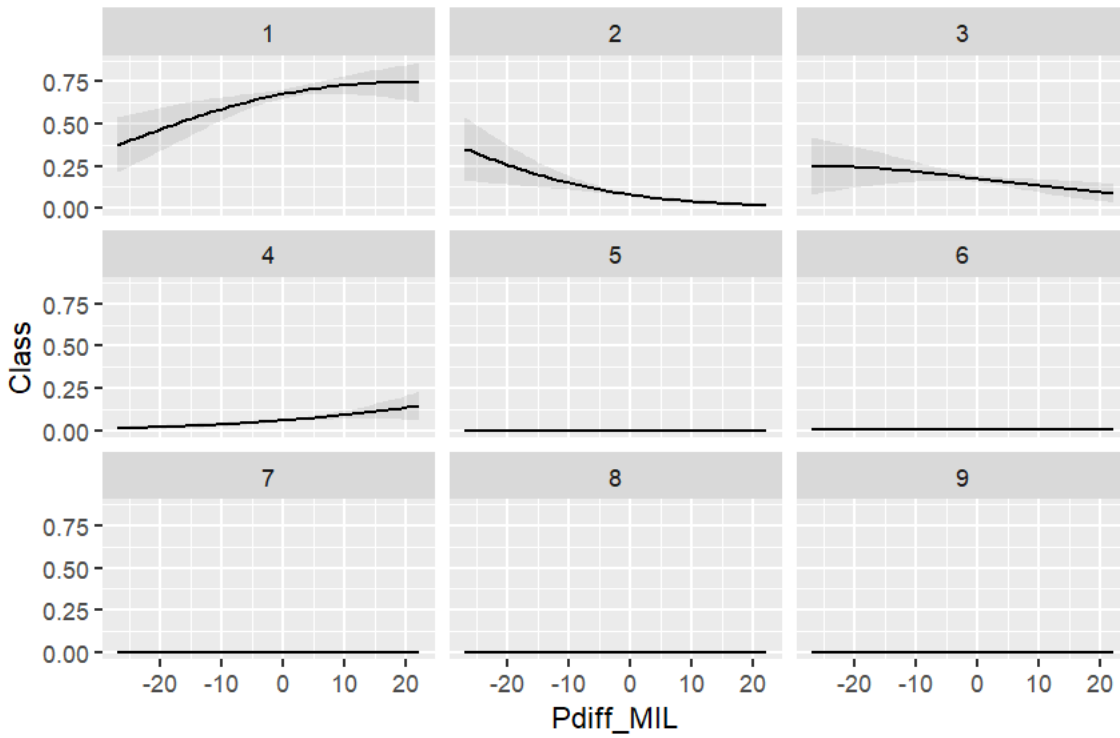


Figure S2.5: As figure S2.1, but for *Pdiff_MIL*.

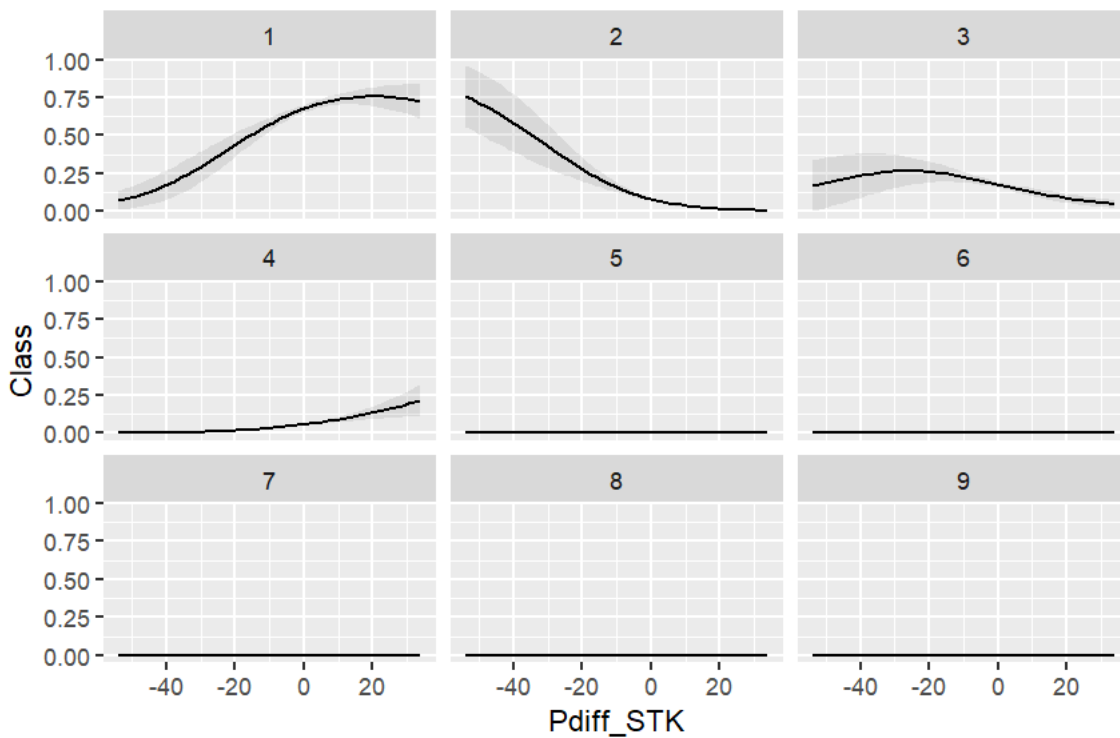


Figure S2.6: As figure S2.1, but for *Pdiff_STK*.

S.3 Random Forests (RF): Feature Importance

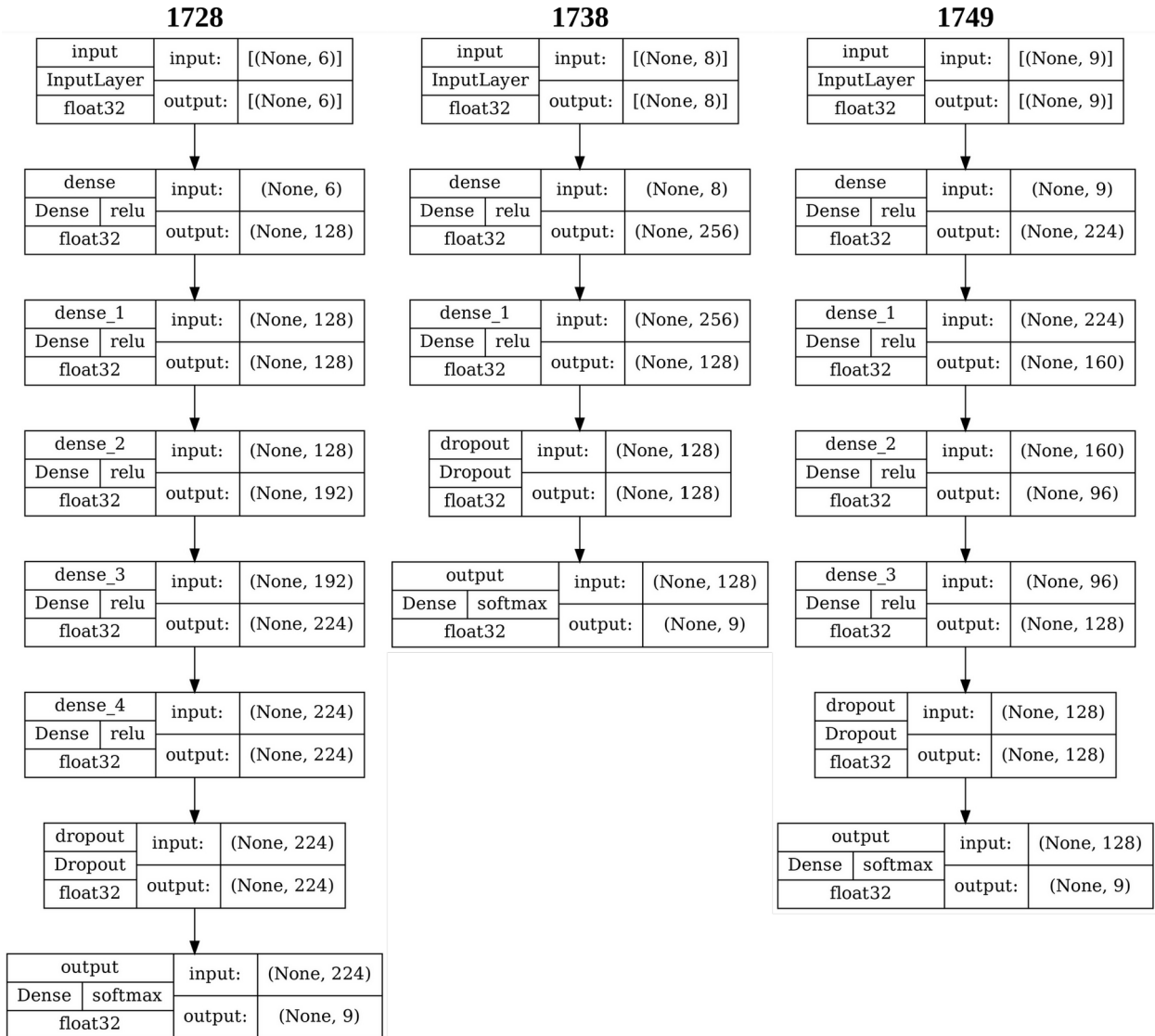
- 20 Feature importance (average reduction of the Gini impurity or entropy in the split classes for each feature (predictor) over all trees) of the random forest input data on the example of the SMD stationset with 11 stations as used by Schwander et al. (2017)

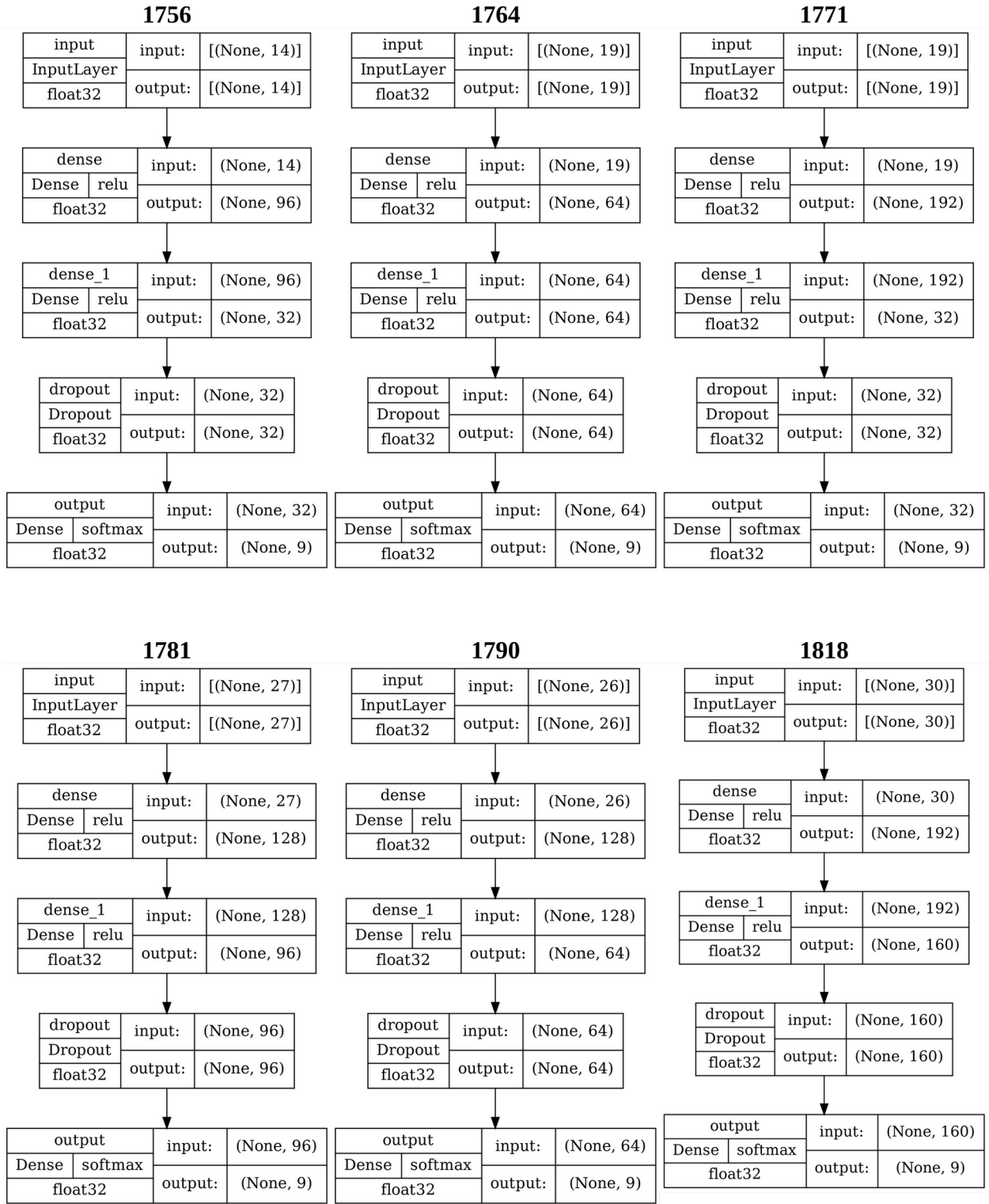
input Variable	feature importance	input Variable	feature importance
PP_LUG	0.1580	TT_SMA	0.0106
PP_MIL	0.1434	TT_TOR	0.0105
PP_DBL	0.1057	TT_PAR	0.0093
PP_BAS	0.0811	TT_UPP	0.0077
PP_SMA	0.0804	TT_STK	0.0075
PP_HPE	0.0712	Pdiff_DBL	0.0069
PP_PAR	0.0606	Pdiff_HPE	0.0067
PP_BER	0.0473	Pdiff_STK	0.0066
PP_LDN	0.0433	Pdiff_MIL	0.0065
PP_STK	0.0139	Pdiff_LDN	0.0063
PP_UPP	0.0127	Pdiff_PAR	0.0063
TT_PRA	0.0119	Pdiff_BAS	0.0061
TT_LUG	0.0118	Pdiff_BER	0.0059
TT_HPE	0.0117	Pdiff_LUG	0.0058
TT_BER	0.0112	Pdiff_UPP	0.0058
TT_MIL	0.0110	Pdiff_SMA	0.0057
TT_BAS	0.0108		

S.4 Neural Network (NN) Architectures

25 Architectures of the best neural network (NN) models for the input data station sets used for the CAP9 reconstructions. They typically contain between 2 and 5 layers (with between 32 and 224 neurons) and (as predefined) a dropout layer. Input and output layers are shown for completeness. The following flowcharts indicate on the left the layer type (in the terminology of the keras library), the activation function (relu or softmax), and the data format, and on the right

30 the size of the input and output of the respective layers. The dimension 'None' represents the variable time dimension.





1864

input	input:	[(None, 35)]
InputLayer		
float32	output:	[(None, 35)]



dense	input:	(None, 35)
Dense relu		
float32	output:	(None, 224)



dense_1	input:	(None, 224)
Dense relu		
float32	output:	(None, 32)

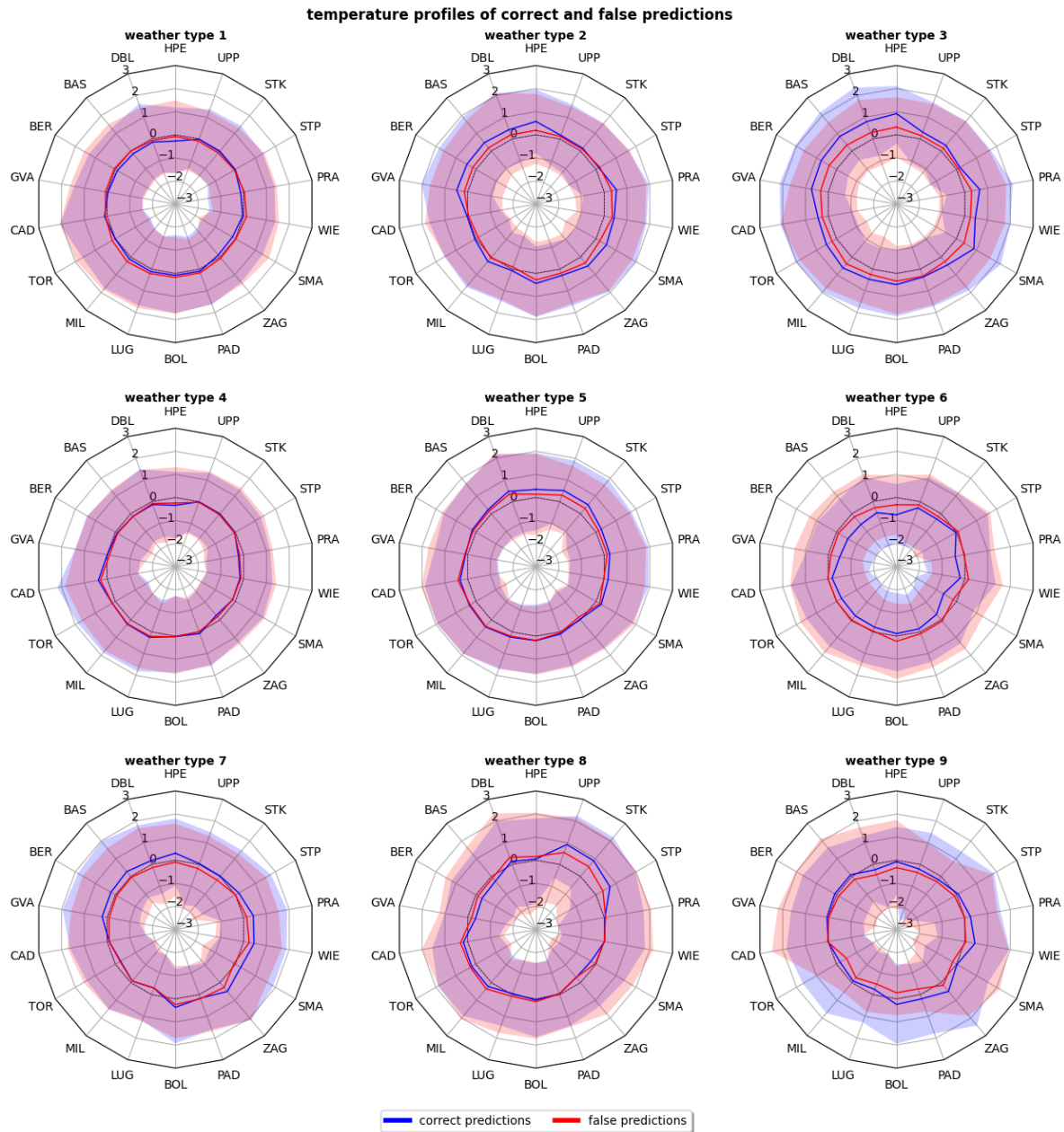


dropout	input:	(None, 32)
Dropout		
float32	output:	(None, 32)



output	input:	(None, 32)
Dense softmax		
float32	output:	(None, 9)

S.5 Additional Analyses of CAP9 Reconstructions



40 **Figure S5.1:** station observation profiles in standard deviations for correctly and wrongly predicted CAP9 weather types as in Fig. 4, but for temperature.

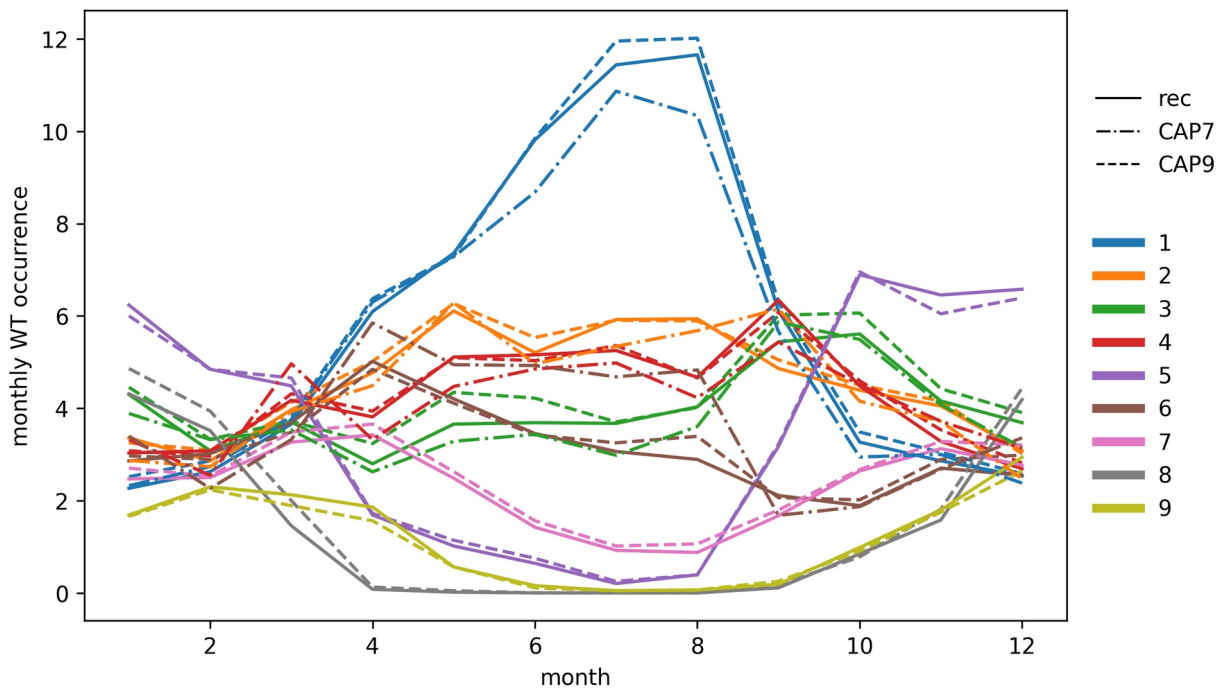


Figure S5.2: average WT seasonality 1957–2020 for reference CAP9 series (dashed line),
 45 CAP9 reconstructions (solid lines), and CAP7 reconstructions (dash-dotted lines, Schwander et
 al., 2017).